Simulation of Dynamic Scattering from Homopolymer and Symmetric Diblock Copolymer Solutions with the Bond Fluctuation Model

Ana M. Rubio, J. Felicity M. Lodge, and Juan J. Freire*

Departamento de Química Física, Facultad de Ciencias Químicas, Universidad Complutense, 28040 Madrid, Spain

Received December 6, 2001; Revised Manuscript Received March 25, 2002

ABSTRACT: The dynamic Monte Carlo algorithm is employed to explore the dynamic scattering of dilute and nondilute solutions of flexible linear chains. The chains are represented by the bond fluctuation model with and without attractions between nonbonded units placed at close distances, to describe different types of thermodynamic conditions (Θ or good solvents). This mimics the behavior of real chains in the different types of solvents. We also consider symmetric diblock copolymer chains in a nonselective good solvent, where the differences between the blocks are introduced in the scattering factors of the beads and, also, through a net repulsion between units belonging to different blocks. The analysis of the dynamic scattering functions for semidilute solutions reveals the presence of at least two different modes. In the homopolymer chains, one of the modes follows the behavior expected for the osmotic mode in the gel regime. The other mode seems to correspond to the structural relaxation, in the case of Θ systems at low values of the scattering, q. At higher q and for good solvents this mode is faster than expected from theory. It can tentatively be assigned to chain end effects. The total intensity at $q = 0$ gives results consistent with the scaling theory for good solvent. The Θ systems show a dramatic increase for this intensity, which is mainly manifested in the slowest collective mode, due to the proximity of critical conditions. For the copolymer chains, we observe a main internal mode, related with the longest Rouse relaxation, and a secondary faster mode that can be due to the accumulation of shorter Rouse motions. The introduction of a moderate repulsion between units in different blocks is manifested through a more prominent peak in the total intensity. Some decrease of the rates is also observed for the same q values, probably caused by the onset of the order−disorder transition.

Introduction

Scattering radiation experiments are currently considered powerful techniques to study the dynamics of a great variety of polymer systems.[1] The "coarse-grained" nature of polymer systems at not very short distances can be adequately monitored through light or neutron experiments. The experiments yield decay curves that, in many cases, can be related with theoretical time−correlation functions generally denoted as dynamic scattering functions.[2] For chains in dilute solutions, these functions can be easily calculated with the simple Rouse or Zimm models.[3] However, the dynamics of semidilute solutions is considerably more complex,[3,4] though many features of the dynamic scattering behavior have been predicted through the application of approximate theories.[5,6] On the other hand, these systems can also be studied by computer simulation.[7] The dynamic trajectories can yield "collective" dynamic scattering functions,[8] directly comparable to the experimental data, and also "intermediate" scattering factors, the latter being the contribution to the scattering from individual chains, averaged on the system. The intermediate scattering factors can be related with experimental neutron scattering from labeled chains or, sometimes, with light-scattering experiments, if the contributing modes are not sensitive to intermolecular interferences.

However, the time scales involved in the simulation of scattering functions are very long and purely dynamic simulations, i.e., molecular dynamics, cannot be practically employed.[7] For this reason, only dynamic Monte Carlo methods with coarse-grained models are presently adequate to accomplish this type of study. These methods rely on the use of "single jump" moves that try to mimic small stochastic perturbations on real polymer beads, and therefore, the choice of a particular coarse-grained model may be important to their actual applicability. Lattice models are particularly useful from the computational point of view, being the only ones that can provide an efficient description of relatively large systems. The choice of elementary moves for individual units is, however, an artificial characteristic of conventional lattice methods. For instance, the simple cubic lattice model has to combine elementary "bents" and "crankshaft" in order to ensure a close-to-ergodic algorithm.[9]

The bond fluctuation model[7,10] was devised to offer the computational benefit of lattices and the more realistic characterization of systems represented by the open space simulations. This model offers a considerably higher number of empty positions available around an occupied site and, furthermore, it only needs a single and simple form of elementary move. These characteristics make this model adequate for Monte Carlo dynamics, especially if interactions between nonbonded units are included, as it is required to study the influence of solvent quality.

In the present article, we report the results obtained for dynamic scattering functions of several different types of many-chain systems in the diluted, semidilute or concentrated regimes. We have considered homopolymer chains in good and Θ solvents. The good solvent systems are represented by self-avoiding walk (SAW) chains. The Θ systems include additional attractions between nonbonded units placed at short distances.[11,12] Also, we have studied symmetric diblock copolymer

10.1021/ma0121262 CCC: $22.00
Published on Web 05/25/2002

chains in a good solvent. The copolymer units A or B belonging to different blocks are distinguished by their different scattering contrast factors. We consider SAW chains in which we have added a net repulsion between A and B units. The model represents the case of diblock copolymers in a common good solvent with moderate block segregation.

This study complements our previous simulations of dynamic scattering for homopolymers in a good solvent[8] and for diblock copolymers without block segregation, both with the simple cubic lattice.[13] These simulations were limited by the large statistical noise of the collective scattering. Now, this problem has been partially overcome due the increase of computational efficiency. Also, in a previous and recent work,[14] we presented a preliminary study of size and some static and dynamic properties of the same homopolymer systems with the present bond fluctuation model. Some of these results are helpful here to complement our discussion of the scattering data.

Simulation Methods

For chains in good solvents, we consider n SAW chains, each composed of N beads, with a set of different possible values of the chain lengths, in a cubic lattice of adequately chosen length,[15] L, including periodic boundary conditions. The distance between adjacent sites, b, is taken as the length unit. Each one of these beads blocks the 26 surrounding lattice sites. Other additional beads (depending on the site position) can also block the 26 sites surrounding a bead. Accordingly, it is easy to verify that a single bead effectively blocks a total of eight sites. Consistently, the required polymer volume fractions is $\Phi = 8nN/L^3$. Other details of the model can be found in ref 14.

Elementary bead jumps are achieved just by randomly moving a bead to one of the six closest sites. This way we generate "dynamic" Monte Carlo trajectories from previously equilibrated samples.[14] In the trajectories, a time unit is constituted by nN subsequently attempted bead jumps. Once a move is attempted, the new bond lengths are checked and the SAW condition is enforced. To do so, we just verify that the new bead position is not blocked by other beads. Consequently, the description of the bond fluctuation model in terms of single site beads given here,[14] though slightly less intuitive than in the original version, is computationally efficient, since it only requires a single site check per move attempt to verify the SAW condition. If any of these checks fails, the move is rejected.

In addition to the SAW condition, we adopt the model proposed by Wittkop et al.[11] to include attractions and bond energies, to describe other types of solvents or bead interactions. The *attractive* interaction energies for the Θ systems are expressed in terms of an energetic parameter $\beta \equiv \epsilon/k_BT$, which corresponds to the absolute value of a negative contribution. Also, we also use the same parameter $\beta \equiv \epsilon/k_BT$ to describe a positive contribution associated with the *repulsive* interaction between A and B units in our copolymer systems. The total energy of a configuration which complies with the self-avoiding condition sums up all the bond energies, together with all the energies corresponding to intramolecular and intermolecular interactions (negative or positive) between pairs of nonneighboring units. The configuration is accepted or not by comparing this "new" energy with the energy of the previous (or "old") configuration, according to the Metropolis criterion. Some further details of the present algorithm are given in our previous work.[14]

For the study of Θ systems, we have considered the value $\beta = 0.214$. This was initially assigned in previous simulations[11] as the Θ point for which the mean size of the chains should proportional to $N^{1/2}$, using a range of chain lengths similar to the present simulations. We have verified that $\beta = 0.2$ is, actually, a better choice,[14] since it gives similar chain sizes at different concentrations and there is not indication of phase separation at any concentration. This conclusion is in agreement with previous simulations performed with a very efficient algorithm for longer single chains.[16] We have also obtained results for this alternative value, but only for $\Phi = 0.15$ and two different chain lengths. In the investigation of copolymers systems, we have considered SAW chains, in which we have included repulsive interactions between A and B units. With this purpose, we also have set $\beta = 0.2$.

The technical parameters of the trajectories (length of trajectories, etc.) were also described in ref 14. All the reported results are referred to two basic units: b (for distance) and a single Monte Carlo step (for time).

The dynamic collective scattering function of the system (or simulation box) can be calculated as

$$S(q,t) = 8n_s^{-1} \langle \sum_i^{n_s} f_i(\tau) f_j(\tau + t) \exp\{i\mathbf{q}[\mathbf{R}_i(\tau) - \mathbf{R}_j(\tau + t)]\} \rangle_\tau \quad (1)$$

and the total intensities, or elastic scattering functions, can be obtained as $A \equiv S(q,t = 0)$. In eq 1, $\boldsymbol{q}$ is the scattering vector, depending on experimental settings, the vectors $\boldsymbol{R}_k(t)$ refer to the positions of the different $n_s = L^3$ sites within the system at time t and $f_k(t)$ is the contrast factor, related to the difference between the scattering factor due to the particular occupation in the site at a given time and the mean scattering factor of the system. Thus, for the homopolymer systems

$$f_i = 1 - \Phi/8 \quad (2a)$$

if site i contains a bead unit, or

$$f_i = -\Phi/8 \quad (2b)$$

otherwise, to comply with the requirement that the global system considered as a single macroscopic volume does not scatter. In this assignment of contrast factors, we have considered that the additional seven sites effectively blocked by any chain bead are "solvent sites". (We cannot easily assign these blocked sites as "polymer beads" since a site can be actually blocked by a changing number of monomer beads.) With the introduction of factor 8 in eq 1, the results should be equivalent to those obtained with the contrast factors of $(1 - \Phi)$ for each blocked site and $-\Phi$ for each nonblocked solvent site. Therefore, we can consistently compare our results with those obtained with the simple cubic lattice model,[17,18] except for values of $q \equiv |\boldsymbol{q}|$ high enough to monitor distances similar or smaller than b.

For the symmetric diblock copolymers, we assume that the solvent scattering factor is equal to the system's mean. In this case

$$f_i = -1 \quad (3a)$$

if site i is occupied by unit A

$$f_i = 1 \quad (3b)$$

if site i is occupied by unit B.

Or, finally,

$$f_i = 0 \quad (3c)$$

if site i is empty or blocked. Also in this case, factor 8 in eq 1 accounts for the smaller scattering density of the polymer beads in our description, due to the "blocked solvent sites" assignment.

The scattering results do not depend on the orientation of vector $\mathbf{q}$ for isotropic samples. In fact, these results can sometimes be conveniently scaled in terms of variable x, defined as

$$x = q^2 \langle S^2 \rangle \quad (4)$$

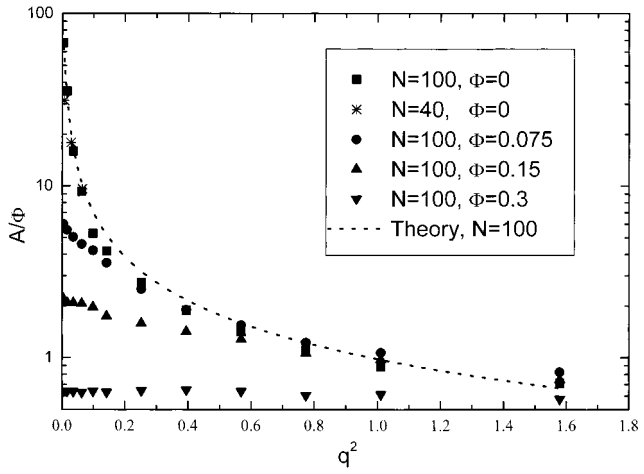

Figure 1. Good solvent systems ($\beta = 0$). Relative total scattering intensities vs q^2 for dilute chains of $N = 100$ and $N = 40$. Broken line: theoretical prediction from eqs 4, 7, and 8, with the values of $\langle S^2 \rangle$ corresponding to the simulation trajectory for $N = 100$.[14] Also, simulation results for $N = 100$ at other concentrations.

where $\langle S^2 \rangle$ is the mean quadratic radius of gyration of the chains. (We will use variable q^2 to present all our scattering results. However, we will discuss some results also in terms of x, when these data are compared with theoretical expressions depending also on chain length through variable x.) The practical range of values of q in the simulations is limited by the periodic boundary condition

$$q_k = (2\pi/L)n_k, \quad k \equiv x,y,z, \quad n_k = 1, 2..., \tag{5}$$

which determines the smallest value of q. On the other hand, high values of q exhibit a very fast decay of the dynamic functions, and the precise determination of fitted parameters becomes difficult. Results for the collective scattering function corresponding to all the possible orientations of vector $\boldsymbol{q}$ are obtained and adequately averaged.

Our simulations cover a wide range of concentrations including dilute (single chains), semidilute, and concentrated, close to melt systems (the latter only for homopolymers in a good solvent). The semidilute regime is reached for concentrations above a critical overlapping value Φ^*, which can be estimated as[4]

$$\Phi^* \cong 8N/(4\pi\langle S^2\rangle_0^{3/2}/3) \tag{6}$$

where $\langle S^2 \rangle_0$ is $\langle S^2 \rangle$ at $\Phi \cong 0$. The overlapping concentrations that correspond to the homopolymer systems were reported in Table 2 of ref 14.

Results and Discussion

(a) Homopolymers in a Good Solvent. In Figure 1, we present the total intensities vs q^2 from the collective scattering function at different concentrations and for the longest chains included in our simulations, $N = 100$, in the case of SAW homopolymer chains (which mimic the behavior in a good solvent). We also show some data corresponding to the dilute $N = 40$ chain. The results for dilute systems can be described as

$$S(q,t) = N\Phi P(x,t) \tag{7}$$

where $P(x,t)$ is the intermediate scattering function, obtained without considering intermolecular scattering interferences. For the intensities, we can consider the Debye which describes the form factor, $P_0(x) = \mathrm{P}(x, t =$ 0) of ideal single homopolymer chains

$$P_0(x) = (2/x^2)(e^{-x} + x - 1) \tag{8a}$$

For high x, excluded volume effects are significant, and we substitute eq 8a by[19]

$$P_0(x) = 1.2599/x^{0.8503} + 1.3057/x^{1.7007} - 1.7432/x^{1.855} - 0.2553/x^{3.0686} \quad x \geq 3.5 \tag{8b}$$

which gives an asymptotic plateau for $P_0(x)x^{1/2\nu}$ consistent with the concentration-independent blob behavior in a good solvent.[4] Agreement is good, with some differences at intermediate and high x due to the model rigidity and finite extension of the chains.[19,20]

For nondilute systems, however, the intensities should decrease with concentration. In the semidilute regime, we expect three distinct behaviors for A. At low x, the curves are flat. This is consistent with the random phase approximation for the total intensity,[21]

$$1/A = 1/\Phi N P_0(q) + (v_e\Phi) \tag{9}$$

(where v_e is the β-dependent excluded volume parameter) if the second term on the right-hand of eq 9 is predominant, due to a significantly high positive value of v_e for $\beta = 0$. Therefore, it is easy to perform an extrapolation to obtain $A(q = 0)$. At higher values of q, the first term in eq 9 becomes more important, and the curves at different concentration tend to converge in order to mimic the behavior of $P_0(x)$, since they are also able to monitor blobs in a good solvent. At still higher values of q, this curve would also show local model features. A detailed study the high q features of intra- and intermolecular structure factors has been recently performed with the same model.[20]

Absence of a blob regime characterizes the concentrated systems. Thus, the curves corresponding to high concentrations ($\Phi = 0.3$, $\Phi = 0.5$) show a rather flat shape for all the values of q. (At very high values of q, these flat curves corresponding to different concentrations are expected to converge to reflect the model local details.) The systems at intermediate concentrations, however, show a moderate decay indicating the slow approach to the blob regime. All our results for the total intensity of nondiluted systems at any given concentration are practically independent of N. Only the dilute systems show a Guinier regime, where $S(q)$ is determined by the reduced variable x at low values of this variable, and therefore, it simultaneously depends on q and the chain size. It can be concluded that the qualitative analysis of the total scattering intensity provides an excellent characterization of the different concentration regimes. (However, other conformational properties, such as the chain size or the translational diffusion coefficient exhibit a more gradual variation with concentration.[14])

We have analyzed the results for $A(q = 0)$ for the nondilute systems. Performing a previous average of the very similar extrapolated data obtained for different N at each concentration, we have carried out log−log linear fits of $S(q = 0)$ vs Φ. We can compare the result with the theoretical prediction[5,6]

$$A(q = 0) = \Phi^2/K \tag{10}$$

where K is the osmotic modulus,[5,6] directly related with the variation of the osmotic pressure with concentration.

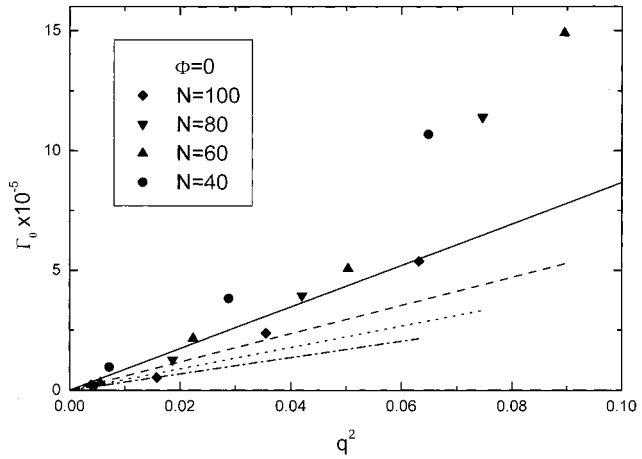

Figure 2. Mode decay rates for a single homopolymer chains of different lengths with $\beta = 0$. The lines show comparison with the theoretical prediction for Γ_0, eq 13, with values of D calculated from the same simulation trajectory[14] (solid, $N = 40$ dash, $N = 60$; dot, $N = 80$; dash−dot, $N = 100$).

Taking into account the scaling law predicted for this variation in a good solvent,[3] we get

$$A(q = 0) \approx \Phi^{1-1/(3\nu-1)} \tag{11}$$

From our simulations, the fitted slope of the log−log representation is −0.65, when all the nondiluted concentrations are included in the fit (with reasonable, but not very good, correlation). If we take only the results for $\Phi = 0.075$ and $\Phi = 0.15$ which correspond to semidilute solutions, we get a slope value of −0.47, in better agreement with the theoretical prediction from eq 11, i.e., with a slope of −0.30 for $\nu = 0.588$. (The consistency of eq 9 with this scaling law requires to assume that parameter v_e depends on concentration. Some technical complications resulting from this scheme at high q are discussed in ref 20.)

The dynamic collective scattering functions obtained from our simulations have been numerically fitted to sums of several exponential functions from which we obtain intensities (from preexponential factors) and decay rates (from the exponent constants) assigned to particular modes. The data corresponding to dilute systems have been adequately fitted to a single exponential. The variation of the decay rates with q^2 is shown in Figure 2. We include the predictions of the Rouse theory

$$P(x,t) \cong P_0(x)\mathrm{e}^{-\Gamma_0 t} \tag{12}$$

where the decay rate corresponds to a diffusive (i.e., linear in q^2) behavior

$$\Gamma_0 \equiv 1/\tau_0 = Dq^2 \tag{13}$$

which are only valid for for low x, with the values of the translational diffusion coefficient previously obtained from the analysis of the same simulation trajectories.[14] It is verified that the rates are consistent with the theoretical prediction. However, the values of q^2 compatible with the simulation parameters mainly correspond to intermediate values of x, and therefore, we can actually observe a gradual deviation from the low x regime to reach the q^4 dependence which corresponds to segmental diffusion.[2,3]

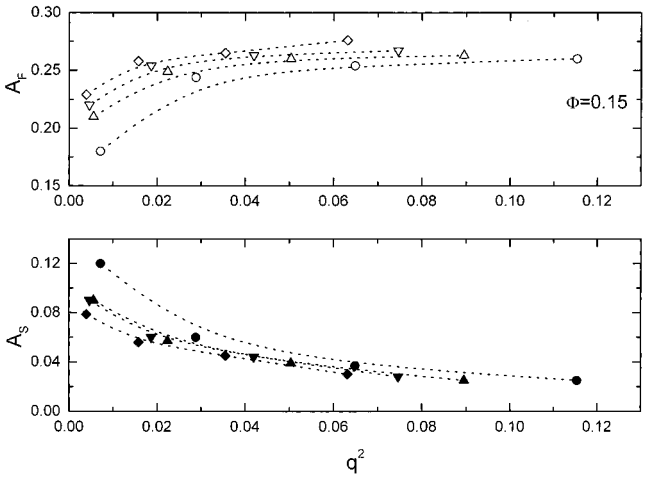

Figure 3. Mode intensities for homopolymer chains at $\Phi = 0.15$, $\beta = 0$. Open symbols represent the fast mode; filled symbols represent the slow mode. Chain length codes for simulation data as in Figure 2. The dotted lines are spline fits.

The data from concentrated solutions ($\Phi = 0.3$ and $\Phi = 0.5$) were also satisfactorily fitted to a single exponential. The fitted decay rates for these systems show a weak dependence on N, q and Φ. The dependence on N decreases for the highest Φ (highest concentration). Our interpretation of these results is that, for concentrated systems, the dynamic scattering can only reflect local changes, essentially fast interchanges of position between a few polymer units, i.e., model-dependent local motions. Diffusive modes are, however, observed in neutron scattering experiments in melts which correspond to higher values of q, reflecting fast motions in the atomic range of distances. Our coarse-grained model cannot describe these motions. The bond fluctuation model has been extensively applied to the study of melts[22] in order to verify the reptation theory. Some of these simulations have actually computed the intermediate scattering function.[23]

The data corresponding to semidilute solutions ($\Phi = 0.075$ and $\Phi = 0.15$) showed a good fit to two exponentials. The results for the semidilute systems can be, in principle, compared with the theoretical predictions.[1,5,6]

$$S(q,t) = [\Phi^2/K(q)][A_S\mathrm{e}^{-t/\tau_S} + A_F\mathrm{e}^{-t/\tau_F}] \tag{14}$$

In general, both intensities and rate decays depend on chain length, concentration and q, as is shown in Figures 3 and 4 for $\Phi = 0.15$. Therefore, we can initially assign the two contributions to the slow (S) and fast (F) modes, corresponding to the smaller and higher decay rates, according to eq 14. The intensity of the fast mode increases moderately at low q, reaching soon a constant value, see Figure 3. The intensity of the slow mode tends to decrease more progressively with q. Therefore, the ratio of the slow and fast mode intensities, A_S/A_F, decreases significantly with q. Eventually it reaches a small constant value at high q. A_S/A_F also decreases with chain length and concentration. The approach to this constant value is faster for the highest values of N and Φ.

These effects could be considered as qualitative, consistent with the theoretical formulation of two modes for the entanglement relaxation in the "gel" regime.[5,6] The fast mode is assigned to osmotic relaxation (fluctuations in solvent concentration) and the slow model is related with structural relaxation (due to the relative

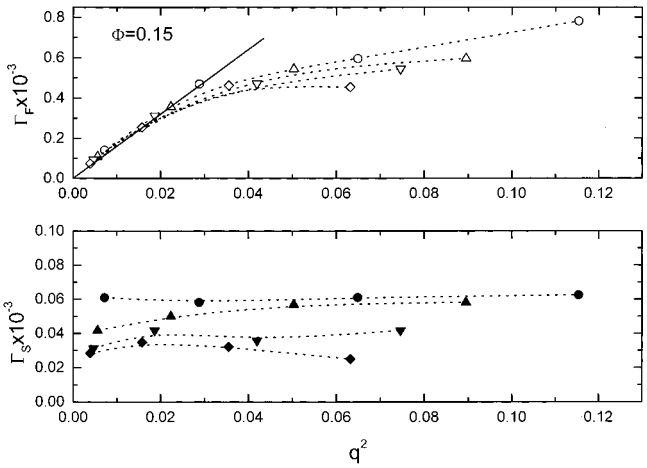

Figure 4. Mode decay rates for homopolymer chains at $\Phi = 0.15$, $\beta = 0$. The solid line is consistent with our estimation of $D_g q^2$. Open symbols represent the fast mode; filled symbols represent the slow mode. Chain length codes are as in Figure 2. The dotted lines are spline fits.

motion between chains). The theory predicts

$$A_S/A_F = \tau_R(D_g/D_c - 1)/(\tau_R - 1/D_g q^2) \qquad (15)$$

where D_g is the gel diffusion coefficient, related to the cooperative diffusion coefficient D_c

$$D_g = D_c(1 + M_g/K) \qquad (16)$$

D_g and D_c are independent of chain length. τ_R is the longitudinal relaxation (or reptation) time of the chains, strongly dependent on chain length and concentration, which determines the formation and destruction of entanglements. M_g is the elastic modulus. For good solvents, however, $K \gg M_g$, and a single mode is experimentally observed. Although it is not clear that the latter condition is effectively preserved in the present simulation model for good solvents, the presence of the slow mode in the simulation data could, therefore, be simply explained by the finite size of the chains. This hypothesis seems to be confirmed by the analysis of rates that will de described below.

The rate of decay for the faster mode, $\Gamma_F = 1/\tau_F$ obeys a universal and diffusive dependence for all the chain lengths when only the two lowest values of q^2 are considered, see Figure 4 (a similar result is found for $\Phi = 0.075$). This feature is in satisfactory agreement with the theoretical description of the fast mode[5,6]

$$\tau_F = (D_g q^2)^{-1}, \qquad (17)$$

Consequently, the linear plots Γ_F vs q^2 yield slopes that can be identified as numerical values of D_g. Since M_g and K should have the same concentration dependences in a good solvent,[6] we can expect that D_c and D_g only differ by a constant (small) factor. On the other hand, D_c should be inversely proportional to the mean size or correlation length of the blobs, ξ.[5,6] Taking into account the scaling law relating ξ with concentration,[4] we obtain

$$D_g \cong D_c \approx \xi^{-1} \approx \Phi^{\nu/(3\nu - 1)} \qquad (18)$$

and our estimates of D_g corresponding to the two different concentrations can be compared with eq 18. We get $D_g = 9.5 \times 10^{-3}$ for $\Phi = 0.075$ and 1.6×10^{-2} for $\Phi = 0.15$. These values give $D_g \approx \Phi^{0.71}$, in good agreement with the theoretical exponent[3,4] $\nu/(3\nu - 1) = 0.77$. A similar agreement with theory is also observed experimentally.[1]

At higher values of q, the decay rates deviate from the diffusive behavior, showing a downward bent and a significant dependence on the chain length. The effects are more noticeable for the highest concentrations. It is possible that the considered values of q correspond to a plateau marking the crossover between the diffusive gel and the internal, or segmental, mode. Since the later mode should not be influenced by concentration, this crossover is conditioned by the difference between D_g and the significantly smaller dilute value $D(c = 0)$, which characterizes the initial diffusive rate in dilute solution, and may be more marked for higher molecular weights and concentrations.

The decay rate of the slower mode, $\Gamma_S = 1/\tau_S$, shows a weaker dependence on q. Actually, it tends to a constant value for high q, and this tendency increases at the highest concentration. The theory predicts a constant value of Γ_S. Also, it predicts that τ_S is proportional to τ_R (and slightly higher). This implies a remarkable decrease of Γ_S with the chain length, which can qualitatively be observed in our data. However, our results for τ_S do not show a significant variation with concentration, in contradiction with the theoretical prediction for τ_R.[4] Moreover, when the numerical results of τ_S are numerically fitted to follow a power dependence with chain length we get $\tau_S \approx N,^{1-2}$ smaller than the theoretical prediction. Our values of τ_S are also 3−10 times smaller than our results for the first Rouse modes, $\tau_1 \approx N,^{2-3}$ obtained directly from the same simulation trajectories.[14] This differences should be considered together with the discrepancies with respect to the theory previously discussed for the intensities. Consequently, we have tried to find an alternative origin for the observed slow mode. A plausible explanation is that this mode actually reflects only the destruction of entanglements due to the motion of the free chain ends (i.e., when only the external parts of the chains is involved in the entanglement). These motions relax more slowly for longer chains and higher concentrations. However, the free ends are shorter at higher Φ, and the net dependence with concentration may be weak. The scattering intensities must decrease with q, but not abruptly, since they correspond to local motions. This mode would not be observable in semidilute solutions of high molecular weight chains. These features are consistent with all the observed trends.

(b) Homopolymers in a Θ Solvent. The total intensities for both $\beta = 0.2$ and $\beta = 0.214$, for $\Phi = 0.15$, and for the presently studied values of q and N were previously reported.[14] They are high and showed a dramatic decrease with q at low q. The data in the form $1/A$ vs q^2 were presented in Figure 2 of ref 14. (There, the ordinates denoted as $S(q)$ actually correspond to $A/8$ in the present notation.) The different sets of data for each given value of β in this figure suggest a linear behavior, showing a small dependence on N and concentration. Slopes of these representations were similar for all cases. The apparent ordinate from the $\beta = 0.2$ data is small and positive, but the ordinate for $\beta = 0.214$ is practically zero, indicating the closer vicinity of spinodal conditions.[4,18] All these features are in agreement with the random phase approximation theory, described by eq 9. This expression, together with eq 4

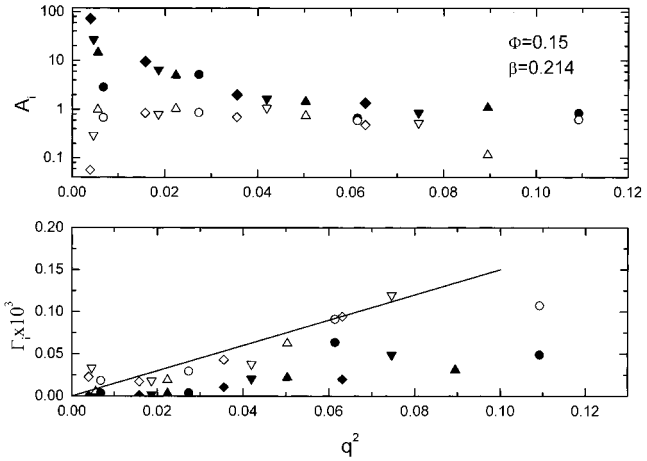

Figure 5. Mode intensities (top) and decay rates (bottom) for homopolymer chains at $\Phi = 0.15$, $\beta = 0.214$. The solid line is consistent with our estimation of $D_g q^2$. Open symbols represent the fast mode; filled symbols represent the slow mode. Chain length codes for simulation data are as in Figure 2.

and an adequate power expansion of the inverse of the Debye function, eq 8a, actually leads to the linear dependence

$$1/A = (1/N\Phi + v_e\Phi) + (a/\Phi)q^2 \qquad (19)$$

(with a small ordinate for $v_e \cong 0$) where, for long chains, a is a numerical constant, depending both on model and also on the particular expansion used for $1/P_0(x)$.

The semidilute results for the Θ systems can be fitted by the sum of two exponentials. However, the variation of the numerical parameters (intensities and rates) with N, Φ, and q is not so clearly defined as for good solvent systems, probably due to numerical difficulties in the separation of the modes, which are now closer in frequency. The variation of the fitted results with q^2 is shown in Figure 5 (for $\Phi = 0.15$, $\beta = 0.214$). The fitting difficulties are clearly apparent for some particular points, where the fitted values of decay rates are closer than it can be expected from a global systematic variation of the data. Consistently anomalous intensities are also observed for the same cases.

Taking as a reference the results for good solvents, it is observed in Figures 5 that the intensities of the slow and fast mode are greater (a similar conclusion is obtained with the smaller concentration $\Phi = 0.075$). The global decrease of the elastic modulus K in eq 14 can explain this effect, which also corresponds to the increase of the total scattering discussed above. Since, according to eqs 9 and 14, $K(q)$ increases with q, the effect is dramatically enhanced in the case of the slow mode, whose intensity must smoothly connect to the intensity of a single mode in the "liquid" regime[5,6] which prevails at $q < 1/(D_g\tau_R)^{1/2}$ (Typically, this regime corresponds to values of q below those of our data).

Regardless of the noisy aspect of the data, it is still possible to recognize the same universal and diffusive q dependence of the fast mode rates found in good solvent. (This region also appears in the Θ data for $\Phi = 0.075$.) In fact, the diffusive behavior now seems to extend to the whole considered interval of q values. It should be considered that these values of q are now monitoring a range of lengths between the blob mean size ξ and the smaller mean distance between binary contacts ξ_e. Rates in this range may still show an N-independent and apparently diffusive behavior.[6] (However, $\xi \cong \xi_e$ in the case of good solvents.) It is also observed that the fast mode rates are remarkably smaller than for the good solvent systems. The estimated values of the gel diffusion coefficients are $D_g \cong 9 \times 10^{-4}$ for $\Phi = 0.075$ and $D_g \cong 1.5 \times 10^{-3}$ for $\Phi = 0.15$, and the variation of these data with concentration is similar to the behavior found for good solvents. According to theory and experimental data,[1,24] we should expect a direct proportionality between D_g and Φ in Θ systems, which, at any rate, is not far from the observed behavior.

The rates of the slow mode show a more complex dependence on q, see also Figure 5. For low values of q, where the slow mode is predominant, these rates are close to zero and the dynamical scattering curves decay very slowly. This implies very large values of τ_S, which are consistent to assign this mode to the slow structure relaxation, though a precise numerical study of these rates cannot be easily accomplished. Consequently, the Θ systems at low q seem to reflect the two modes as predicted by the theory and shown by experiments.[24,25] It should be considered that the decrease in D_c due to the decrease of solvent quality is stronger than the increase found for the first Rouse relaxation time[14] and, presumably, of τ_R in eq 15, leading to a stronger contribution of the slow mode at low q. For higher values of q, however, the rates become similar to those previously obtained in good solvents, also showing a remarkable dependence on the chain lengths. Since the theory predicts an abrupt decrease of the elastic mode with q, the apparent slow mode at higher q may reflect again chain end effects. At low q, this latter mode related with end effects may also be present, since it would be difficult to separate from the fast mode. Some of the decays fits actually suggest the presence of three modes.

We have also analyzed a pair of trajectories corresponding to $\beta = 0.2$ (higher temperature), $\Phi = 0.15$, $N = 40$, 100. According to the previous data, this choice of β reflects better the Θ behavior of long chains or nondilute systems.[14,16] Again, the data are noisy since the decay rates have not adequately separated by the fits in some cases. The intensity of the slow mode at low q becomes significantly lower than for $\beta = 0.214$. This remarks the strong influence of temperature changes (reflected in the excluded volume parameter, v_e) on the osmotic compressibility and K for Θ systems close to the critical behavior, as it follows from eqs 9 and 14. However, the slow mode for $\beta = 0.2$ is still clearly predominant and much higher than for good solvents. It is observed that the gel diffusion coefficient obtained from the fast mode is increased to the value $D_g \cong 2 \times 10^{-3}$. The increase of K, which favors gel diffusion, is also manifested in this feature. The slow mode rates show an earlier increase with q with respect to the $\beta = 0.214$ case. Other features are as for $\beta = 0.214$.

(c) Copolymers. From our new trajectories for the symmetric diblock copolymer model (including repulsions between A and B units) we have obtained the chain size (mean-squared radius of gyration), translational diffusion coefficient and first (longest) Rouse relaxation times at different concentrations. The results are shown in Table 1, and are of the same order of magnitude than the data previously obtained for SAW chains,[14] only showing a modest increase in size (which

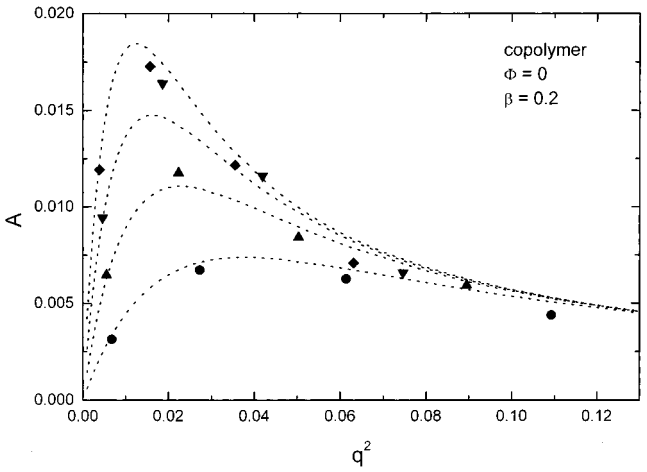

Figure 6. Mode intensities for a single copolymer chains of different lengths with $\beta = 0.2$. Chain length codes for simulation data as in Figure 2. The dotted lines show the intensity predicted by eqs 4, 7, 8, 21, and 22. The values of $\langle S^2 \rangle$ and ν_S (eq 20) correspond to the same simulation trajectories; see Table 1.

Table 1. Values of the Radius of Gyration, $\langle S^2 \rangle$, Translational Diffusion Coefficient, D, and the First (Longest) Rouse Relaxation Times, τ_1, Exponent ν_S (Eq 20), and Overlapping Concentrations (from the $\langle S^2 \rangle_0$ Data) for Copolymers with Repulsive Interactions between the Different Blocks, $\beta = 0.2$

Φ	N	$\langle S^2 \rangle$	$D \times 10^4$	$\tau_1 \times 10^{-4}$	ν_S	Φ*
0.15	100	234	1.22	41.1		
0.15	80	180	1.55	23.0		
0.15	60	130	2.52	14.5		
0.15	40	84	4.15	5.0		
0.15					0.56	
0.075	100	257	1.65	28.0		
0.075	80	200	2.42	17.2		
0.075	60	145	2.92	10.2		
0.075	40	92	4.82	4.1		
0.075					0.60	
0.0	100	309	3.00	26.1		0.035
0.0	80	238	4.42	14.4		0.042
0.0	60	168	5.52	7.9		0.052
0.0	40	102	9.33	3.1		0.074
0.0					0.61	

are related with slightly smaller diffusion coefficients and slightly higher relaxation times) due to segregation between the blocks. The fitted exponents to the scaling law

$$\langle S^2 \rangle \approx N^{2\nu_S} \tag{20}$$

(also shown in Table 1, together with the overlapping concentrations for different chain lengths) are similar to the values of ν_S obtained for the homopolymer chains in good solvents.[14] This indicates that the block segregation effects only alter the proportionality constant in eq 20.

We have also obtained and analyzed the collective dynamic scattering functions (considering opposite contrast factors for A and B units). Figures 6 and 7 show the dependence on q^2 of intensities and decay rates corresponding to dilute copolymer chains with $\beta = 0.2$, whose decays were satisfactorily fitted to a single exponential. The intensities obtained from the simulations are consistent with eq 7, but substituting $P(x,t)$ by $P_{copo}(x,t)$. The copolymer form factor, $P_0^{copo}(x) \equiv$

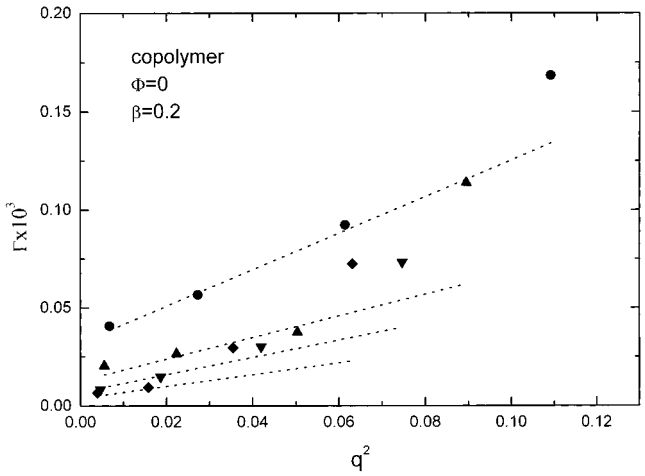

Figure 7. Mode frequencies for single copolymer chains of different lengths at $\beta = 0.2$. Chain length codes for simulation data as in Figure 2. The dotted lines represent Γ_{int} from eq 24, with the values of D and τ_1 corresponding to the same simulation trajectories; see Table 1.

$P_{copo}(x,t=0)$ for single and ideal chains can be obtained as

$$P_0^{copo}(x) = P_0[x(N/2)] - P_0[x(N)] \tag{21}$$

which is actually applied by using eq 20 to obtain the relationship

$$x(N/2) = x(N)/2^{2\nu_S} \tag{22}$$

(eq 8 is introduced in the two terms of eq 21 to describe the form factors; the agreement with the theory at relatively low x is not significantly altered by the different set of interactions considered for the copolymer chains.) As predicted by the theory, the intensities show a maximum at intermediate values of q^2 or x. This maximum is associated with the block size, and therefore, it is located at lower q for longer chains.

The rates shown in Figure 7 exhibit a nondiffusive behavior, with a small, though distinguishable, positive slope. The application of the Rouse chain theory to an ideal and symmetric single diblock copolymer chain (with opposite contrast factors for A and B) shows that, for low or moderate values of x[26]

$$P_{copo}(x,t) \cong P_0^{copo}(x) e^{-\Gamma_{int} t} \tag{23}$$

with

$$\Gamma_{int} = Dq^2 + 1/\tau_1 \tag{24}$$

The values at $q = 0$ are associated with the inverse of the first Rouse mode relaxation times and the slopes are associated with the translational diffusion coefficients, according to the data shown in Table 1. As in the dilute homopolymer chains, the deviations from this linear behavior at higher q are caused by faster internal or segmental modes, which also contribute at intermediate values of x.

As in the case of homopolymers, the copolymer dynamic scattering data for semidilute solutions are also adequately fitted by the sum of two exponentials. However, their values and their dependence on q differ from those found for homopolymers. The results for

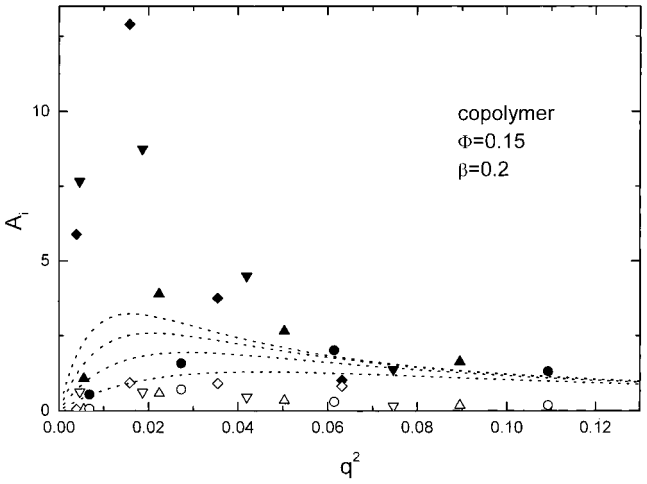

Figure 8. Mode intensities for copolymer chains at $\Phi = 0.15$, $\beta = 0.2$, also showing the theoretical predictions for the total intensity calculated as in Figure 6, with the values of $\langle S^2 \rangle$ and ν_S corresponding to the same simulation trajectories, see Table 1 (dotted lines). Open symbols represent the fast mode, filled symbols represent the slow mode. Chain length codes for simulation data as in Figure 2.

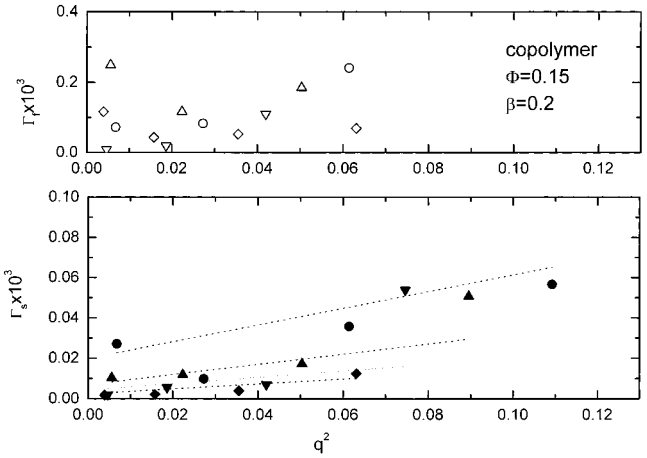

Figure 9. Mode decay rates for copolymer chains at $\Phi = 0.15$, $\beta = 0.2$. In the lower part of the figure, the slow mode is shown with the theoretical prediction for Γ_{int} from eq 24, with the values of D and τ_1 corresponding to the same simulation trajectory, see Table 1 (dotted lines). Open symbols represent the fast mode, filled symbols represent the slow mode. Chain length codes for simulation data are as in Figure 2.

intensities and rates at $\Phi = 0.15$ are given in Figures 8 and 9. In Figure 8, we can distinguish between a predominant mode, with a maximum at intermediate q, and a faster mode, whose intensity is relatively small and increases at higher q. Comparing these results with those obtained for $\Phi = 0.075$, a strong increase of intensities with concentration is also observed. This constitutes a significant difference with respect to the behavior observed for the semidilute homopolymer chains.

Examination of the intensity of the predominant mode reveals that, in fact, for higher concentrations, there is an increasing intermolecular segregation between different block for the systems with repulsion between A and B units. This effect is clearly shown in Figure 8, when we can observe that the mode intensity is considerably higher than the theoretical prediction for total intensity, calculated as in the case of dilute solutions. It should be mentioned that we have also evaluated $S(q,t)$ from eq 1, taking the copolymer contrast factors from eq 3, but using the trajectories corresponding to the semidilute homopolymers in a good solvent (i.e., the $\beta = 0$ systems). This way, we mimic the behavior of copolymer from the scattering point of view, without considering segregation between units. We obtain again two modes, similar to those found for the copolymers with repulsions between A and B units. However, the total intensities agree with the predictions of the elementary theory in this case, confirming that their increasing deviations found for $\beta = 0$ are only due to block segregation.

According to Figure 9, the behavior of the rates corresponding to the predominant mode at low q^2 is reasonably well described by eq 24 with the values of D and τ_1 corresponding to each particular system and contained in Table 1. However, we can observe the deviations at higher q also shown by the global rates of the dilute chains. Our assignment of opposite contrast factors for the A and B units and zero contrast factor for empty (or solvent) sites can, in principle, eliminate modes which do not correspond with the concerted motion of A and B units. Since A and B are maintained together exclusively by the presence of a junction bond within the chains, we should only expect modes corresponding to internal motions of all the individual chains, without important intermolecular contributions. Therefore, the predominant contribution should be associated with the internal mode[27,28] predicted from the random phase approximation and the linear response theories.

A more detailed observation of some of the rates of the predominant mode in the region of q values close to the total intensity maximum suggests, however, a decrease in this region, more significant for the case $\Phi = 0.15$, shown in Figure 9, than for the more dilute system with $\Phi = 0.075$. (Although some oscillations are also apparent due to statistical noise, similar minima are not systematically found from the trajectories obtained for the $\beta = 0$ systems.) This effect may correlate with the approach to an order−disorder transition (ODT). This transition is associated with the formation of lamellar mesophases in concentrated solutions or melts.[29] It is expected that, in the vicinity of ODT, a decrease of the rates should be observed, in conjunction with the increase of intensities in the maximum region, being both features described by global variable $N\Phi\beta$. This behavior has been observed experimentally.[28,30] Despite this more complex feature, it is apparent that the rate corresponding to the main internal mode shows the previously analyzed moderate increase due to the translational diffusion contribution at low q. This increase is not explicitly predicted by the theoretical descriptions for semidilute solutions at low x.[27,31]

The low intensity mode can also be an alternative effect of the accumulation of shorter internal motions. Our previous study of intermediate scattering functions of SAW copolymers, represented by the simple cubic lattice model,[13] also detected this second mode at intermediate values of x. Its presence is conditioned by interactions with the surrounding chains, since we have also previously verified that the decays of the intermediate scattering functions deviate more significantly from the single-exponential behavior for systems beyond the overlapping concentration.[32] Consistently with this assignment, this mode is nondiffusive and shows a noticeable increase with q with the apparent presence of a peak at higher values of q.

Furthermore, we should also remark that, even in the considered regime away from ODT, the experimental data show more complex decays,[30,33,34] with the presence of at least an additional diffusive mode, due to the heterogeneity of the relative distribution of block lengths in different individual chains. This feature was explicitly incorporated and analyzed in our previous simulations[13] and has not been considered in the present study. The experimental data of nondilute copolymer systems in good solvents also show a faster collective mode, unless the contrast factor of the solvent is exactly matched with the system's mean value.[34] This additional collective mode is equivalent to the fast mode shown by the homopolymer chains in the present study.

Acknowledgment. This work has been supported by the TMR European Network Project "NEWRUP". Grant PB98-0791 from the DGESIT, Ministerio de Educación y Cultura, Spain, is also acknowledged. We acknowledge useful discussion with Prof. Arturo López Quintela (Universidad de Santiago de Compostela, Spain). J.J.F. carried out the final steps of the manuscript preparation at the "Departamento de Ciencias y Técnicas Experimentales, Universidad Nacional de Educación a Distancia", Madrid, Spain.

References and Notes

(1) Brown, W., Ed. *Dynamic Light Scattering*; Clarendon: Oxford, England, 1993.
(2) Berne, B.; Pecora, R. *Dynamic Light Scattering*; Wiley: New York, 1977.
(3) Doi, M.; Edwards, S. *The Theory of Polymer Dynamics*; Clarendon: Oxford, England, 1986.
(4) de Gennes, P.-G. *Scaling Concepts in Polymer Physics*; Cornell: Ithaca, NY, 1979.
(5) Brochard, F.; de Gennes, P.-G. *Macromolecules* **1977**, *10*, 1157.
(6) Adam, M.; Delsanti, M. *Macromolecules* **1985**, *18*, 1760.
(7) Binder, K., Ed. *Monte Carlo and Molecular Dynamics Simulations in Polymer Science*; Oxford University Press: New York, 1995.
(8) López Rodríguez, A.; Rey, A. Freire, J. J. *Macromolecules* **1992**, *25*, 3266.
(9) Boots, H.; Deutch, J. M. *J. Chem. Phys.* **1977**, *67*, 4608.
(10) Carmesin, I.; Kremer, K. *Macromolecules* **1988**, *21*, 2819.
(11) Wittkop, M.; Kreitmeier, S.; Göritz, D. *J. Chem. Phys.* **1996**, *104*, 3373.
(12) Wilding, N. B.; Müller, M.; Binder, K. *J. Chem. Phys.* **1996**, *105*, 802.
(13) Molina, L. A.; Freire, J. J. *J. Chem. Phys.* **1998**, *109*, 2904.
(14) Rubio, A. M.; Lodge, J. F. M.; Storey, M.; Freire, J. J. *Macromol. Theor. Simul.* **2002**, *11*, 171.
(15) Kremer, K. *Macromolecules* **1983**, *16*, 1632.
(16) Grassberger, P. *Phys. Rev. E* **1997**, *56*, 3682.
(17) Sariban, A.; Binder, K. *Colloid Polym. Sci.* **1989**, *287*, 468.
(18) López Rodríguez, A.; Freire, J. J.; Horta, A. *J. Phys. Chem.* **1992**, *96*, 3954.
(19) Bishop, M.; Alvarez, G.; Bishop, M. *Macromol. Theor. Simul.* **2002**, *11*, 9.
(20) Müller, M.; Binder, K.; Schäfer, L. *Macromolecules* **2000**, *33*, 4568.
(21) Benoit, H.; Benmouna, M. *Polymer* **1984**, *25*, 1059.
(22) Paul, W.; Binder, K.; Heerman, D. W.; Kremer, K. *J. Chem. Phys.* **1991**, *95*, 7726.
(23) Wittmer, J.; Paul, W.; Binder, K. *J. Phys. II* **1994**, *4*, 873.
(24) Nicolai, T.; Brown, W.; Johnsen, R. M.; Stepanek, P. *Macromolecules* **1990**, *23*, 1165.
(25) Nicolai, T.; Brown, W.; Hvidt, S.; Heller, K. *Macromolecules* **1990**, *23*, 5088.
(26) Rey, A.; Freire, J. J. *J. Chem. Phys.* **1994**, *101*, 2455.
(27) Akcasu, A.; Benmouna, M.; Benoit, H. *Polymer* **1986**, *27*, 1935.
(28) Boudenne, N.; Anastasiadis, S. H.; Fytas, G.; Xenidou, M.; Hadjichristidis, N.; Semenov, A. N.; Fleicher, G. *Phys. Rev. Lett.* **1996**, *77*, 506.
(29) Hamley, J. W. *The Physics of Block Copolymers*; Oxford University Press: Oxford, England, 1998.
(30) Chrissopoulou, K.; Pryamitsyn, V. A.; Anastasiadis, S. H.; Fytas, G.; Semenov, A. N.; Xenidou, M.; Hadjichristidis, N. *Macromolecules* **2001**, *34*, 2156.
(31) Semenov, A. N.; Anastasiadis, S.; Boudenne, N.; Fytas, G.; Xenidou, M.; Hadjichristidis, N. *Macromolecules* **1997**, *30*, 6280.
(32) Molina, L. A.; Freire, J. J. *J. Chem. Phys.* **1996**, *104*, 2093.
(33) Pan, C.; Mauer, W.; Liu, Z.; Lodge, T. P.; Stepanek, P.; von Meerwall, E. D.; Watanabe, H. *Macromolecules* **1995**, *28*, 1643.
(34) Liu, Z.; Pan, C.; Lodge, T. P.; Stepanek, P. *Macromolecules* **1995**, *28*, 3221.

MA0121262